

INVESTIGATING THE NATURE OF ABSORPTION LINES IN THE *CHANDRA* X-RAY SPECTRA  
OF THE NEUTRON STAR BINARY 4U 1820–30E. M. CACKETT<sup>1,2</sup>, J. M. MILLER<sup>1</sup>, J. HOMAN<sup>3</sup>, M. VAN DER KLIS<sup>4</sup>, M. MÉNDEZ<sup>4,5,6</sup>,  
J. RAYMOND<sup>7</sup>, D. STEEGHS<sup>7</sup>, R. WIJNANDS<sup>4</sup>*Submitted to ApJ*

## ABSTRACT

We use four *Chandra* gratings spectra of the neutron star low-mass X-ray binary 4U 1820–30 to better understand the nature of certain X-ray absorption lines in X-ray binaries, including the Ne II, Ne III, Ne IX, O VII, and O VIII lines. The equivalent widths of the lines are generally consistent between the observations, as expected if these lines originate in the hot interstellar medium. No evidence was found that the lines were blueshifted, again supporting the interstellar medium origin, though this may be due to poor statistics. There may be low-level variability in the O VIII Ly $\alpha$  line though it is not clearly correlated with the source flux as might be expected if the origin of the line is local to the source. We conclude that a high fraction of the absorption is interstellar in origin, but more sensitive observations are needed to search for low-level variability.

*Subject headings:* accretion, accretion disks — stars: neutron — X-rays: individual (4U 1820–30) — X-rays: binaries — X-rays: ISM

## 1. INTRODUCTION

High-resolution X-ray spectroscopy from *Chandra* and *XMM-Newton* allows for the study of absorption and emission lines in Galactic X-ray binaries. While emission lines are clearly associated with the sources themselves (e.g., Cottam et al. 2001a,b; Schulz et al. 2001), that is not always the case for absorption lines. In some systems, the absorption lines are also clearly associated with the source, as they are observed to be variable and/or blueshifted (e.g., Lee et al. 2002; Parmar et al. 2002; Ueda et al. 2004; Boirin et al. 2005; Díaz Trigo et al. 2006; Miller et al. 2006a,b). However, in other sources the lines are interpreted as being associated with absorption by the hot ionized interstellar medium, which is thought to be present in the disk and halo of the galaxy, with temperatures around 10<sup>6</sup> K (e.g., Futamoto et al. 2004; Yao & Wang 2005; Juett et al. 2006, and references therein).

From studies of the absorption lines in the black hole X-ray binary GRO J1655–40, the plethora of highly-ionized lines that are detected are all seen to be blueshifted – evidence for a mass outflow into our line of sight, presumably from the accretion disk. In fact, detailed modeling of the lines in this system suggest that magnetic fields may be the force driving the wind (Miller et al. 2006a). Other black hole systems also show evidence for highly-ionized outflows such as H 1743–322, GX 339–4 and GRS 1915+105 (Miller et al. 2006b, 2004; Lee et al. 2002). Disk winds are also observed from the accretion disks around supermassive black holes in Active Galactic Nuclei, e.g. NGC 3783 (see

Chelouche & Netzer 2005, and references therein).

Several neutron star low-mass X-ray binaries also display clear evidence for absorption local to the source. For example, GX 13+1 shows blueshifted absorption lines indicating an outflow with a velocity of  $\sim$ 400 km s<sup>-1</sup> (Ueda et al. 2004). Moreover, in the X-ray dipping sources, strong absorption lines are observed as these objects are inclined close to the orbital plane (e.g., Sidoli et al. 2001; Parmar et al. 2002; Boirin et al. 2005; Church et al. 2005; Díaz Trigo et al. 2006). On the other hand, the nature of the absorption lines observed in many other neutron star X-ray binaries is less clear – the lines are weaker and there is no evidence of significant blueshifts, supporting the interpretation that these lines are due to the interstellar medium (e.g., Yao & Wang 2005; Juett et al. 2006).

As part of the *Chandra* HETGS Z/Atoll Spectroscopic Survey (CHAZSS) we have obtained sensitive observations of 6 neutron star low-mass X-ray binaries at 2 separate epochs using the *Chandra* high energy transmission grating spectrometer (HETGS). The multiple epochs allow for a search for variability in the absorption lines present in these systems; this is key for learning about the nature of the absorption lines. In this paper, we present the observations of the system 4U 1820–30 from this survey. Tight limits can be set on the size of any absorbing region associated with a binary if the system is ultra-compact in nature. Therefore, the ultra-compact nature of 4U 1820–30 (Stella, Priedhorsky, & White 1987) makes it a particularly interesting source to study absorption lines.

2. PREVIOUS *CHANDRA* OBSERVATIONS OF  
4U 1820–30

4U 1820–30 is an accreting neutron star low mass X-ray binary in the globular cluster NGC 6624, which has a well determined distance ( $7.6 \pm 0.4$  kpc Kuulkers et al. 2003) and reddening ( $E(B-V) = 0.32 \pm 0.03$  Kuulkers et al. 2003; Bohlin et al. 1978). This reddening is consistent with the total HI column density of our Galaxy in this direction determined from 21 cm radio observations,  $N_H = 1.5 \times 10^{21}$  cm<sup>-2</sup> (Dickey & Lockman 1990). We adopt the above column den-

Electronic address: ecackett@umich.edu

<sup>1</sup> Department of Astronomy, University of Michigan, 500 Church St, Ann Arbor, MI 48109-1042, USA<sup>2</sup> Dean McLaughlin Postdoctoral Fellow<sup>3</sup> MIT Kavli Institute for Astrophysics and Space Research, MIT, 70 Vassar Street, Cambridge, MA 02139-4307<sup>4</sup> Astronomical Institute ‘Anton Pannekoek’, University of Amsterdam, Kruislaan 403, 1098 SJ, Amsterdam, the Netherlands<sup>5</sup> SRON - Netherlands Institute for Space Research, Sorbonnelaan 2, 3584 CA Utrecht, the Netherlands<sup>6</sup> Astronomical Institute, University of Utrecht, PO Box 80000, 3508 TA Utrecht, The Netherlands<sup>7</sup> Harvard-Smithsonian Center for Astrophysics, 60 Garden Street, Cambridge, MA 02138, USA

TABLE 1  
*Chandra* OBSERVATIONS OF 4U 1820–30

ObsID	Observation Date	Grating/Detector	Exposure (ks)
98	2000 Mar 10	LETG/HRC	15.12
1021	2001 Jul 21	HETG/ACIS	9.70
1022	2001 Sep 12	HETG/ACIS	10.89
6633	2006 Aug 12	HETG/ACIS	25.18
6634	2006 Oct 20	HETG/ACIS	25.13

NOTE. — ObsID 6633 and 6634 are the new observations presented in this work.

sity throughout this paper.

Absorption lines and edges in the X-ray spectrum of this source have been studied previously by Futamoto et al. (2004), Yao & Wang (2005) and Yao & Wang (2006) using an LETG/HRC *Chandra* observation (ObsId 98), and by Juett et al. (2004), Yao & Wang (2005), Juett et al. (2006) and Yao & Wang (2006) using HETG/ACIS *Chandra* observations (ObsIds 1021 and 1022). A summary of the *Chandra* observations of this source is given in Table 1. We briefly summarize the main results of these previous studies below.

Futamoto et al. (2004) clearly detect the O VII He $\alpha$ , O VIII Ly $\alpha$ , and Ne IX He $\alpha$  absorption lines in the LETG spectrum, and put upper limits on the O VII He $\beta$  line. From their curve of growth analysis and photoionization modeling, they deduce that all oxygen will be fully photoionized if the absorbing column is located close to the binary system, and therefore attribute these lines to hot gas in the ISM. However, we note that they make two tacit assumptions - that the filling factor of the gas is 1, and that all the absorption arises from the same gas.

The studies by Juett et al. (2004) and Juett et al. (2006) are concerned with the absorption edges from oxygen, neon and iron, comparing the spectra of a number of X-ray binaries. In Juett et al. (2004) the structure around the oxygen edge in 7 X-ray binaries is studied, looking at the O I, O II, and O III absorption lines in that region. The edge and these low ionization lines are attributable to ISM absorption. In Juett et al. (2006) the neon and iron L edges are studied, and the nature of the neon absorption lines discussed. These authors come to the conclusion that the neon lines in the low-mass X-ray binaries studied are consistent with predictions for the ISM, except for the Ne IX line detected in the black hole X-ray binary GX 339–4 Miller et al. (2004) which shows a column density significantly higher than predicted for the ISM, confirming that the largest contribution to this line (in this source, at least) is from local absorption.

From a study of 10 low-mass X-ray binaries, Yao & Wang (2005) find that the detected Ne IX, O VII and O VIII absorption lines are consistent with the hot ISM origin. Yao & Wang (2006) focuses specifically on 4U 1820–30, discussing the implications of the Ne and O abundance in the ISM from the absorption lines/edges in the *Chandra* observations.

### 3. OBSERVATIONS AND DATA REDUCTION

All the previous observations discussed above suffer from pileup, where a high count rate leads to more than one photon arriving at a pixel per read out. This affects the shape of the spectrum, typically making it harder as the sum of the energies of the multiple photons that arrived between each readout is detected as one count. It is unclear how pileup affects the measurement of absorption lines. It likely modifies the continuum level and shape, which would in turn change any

measured equivalent widths (which depends on the continuum flux across the line). Currently, there is no unambiguous way to model pileup in *Chandra* gratings spectra. To minimize pileup we operated *Chandra* with the High Energy Transmission Grating Spectrometer in continuous clocking mode to significantly increase the temporal resolution. Continuous clocking mode allows milli-second timing at the expense of one dimension of spatial information.

As part of CHA $\zeta$ SS, 4U 1820–30 was observed twice with *Chandra* for approximately 25 ksec each time, first on 2006 Aug 12 (ObsId 6633), and later on 2006 Oct 20 (ObsId 6634). The HETGS-dispersed spectrum was read-out with the ACIS-S array operating in continuous-clocking mode. We reduced these data using CIAO version 3.3.0.1 and following the standard analysis threads<sup>8</sup>. Using the *tgextract* tool spectra the +1 and -1 order were extracted at the nominal instrument resolution for both the high-energy grating (HEG) and the medium-energy grating (MEG). Using the standard redistribution matrix files (RMFs) from the CALDB, the ancillary response files (ARFs) were generated using the *fullgarf* script. We carefully inspected the MEG +1 and -1 orders to confirm there was no wavelength shift between the two orders. The spectra and ARFs were then added together using the *add\_grating\_spectra*, giving a first-order spectrum for the MEG. Similarly, we created a first-order spectrum for the HEG.

In addition to analyzing these two new *Chandra* observations, we also re-analyze the two previous *Chandra* HETGS observations of 4U 1820–30 (ObsId 1021 & 1022) to allow for a search for variability in the absorption lines. These two datasets were not operated in continuous-clocking mode, and suffer from pile-up. We reduce the data following the standard analysis threads, extracting the spectra and ARFs using the same method described above. For consistency, we only analysis the HETGS observations here and not the LETGS observation which has a lower spectral resolution.

## 4. ANALYSIS AND RESULTS

### 4.1. Absorption lines

When searching for absorption lines, we use only the MEG spectra, as the MEG has a higher effective area over the region of interest compared to the HEG. We inspected the spectra over 2 $\text{\AA}$  segments from 2 $\text{\AA}$  to 24 $\text{\AA}$  using the ISIS spectral fitting package. In each segment, we fitted a simple power-law (modified, where appropriate, by an absorption edge due to neutral elements in the ISM). Within each segment, we searched for any significant absorption lines present. We fitted a Gaussian to the detected absorption lines whose central wavelength, width, and normalization were all allowed to be free parameters. The equivalent width of the line was determined from the fitted Gaussian. For line identifications we use Verner, Verner, & Ferland (1996) as a reference. However, for Ne II and Ne III we use the wavelengths determined by Juett et al. (2006). They find the weighted mean of the central wavelengths of these lines measured in multiple X-ray binaries. The wavelengths for these lines from different sources are seen to consistent with each other, and are all systematically shifted by a small amount ( $\sim$ 20m $\text{\AA}$ ) from the theoretical value determined by Behar & Netzer (2002), though within their stated errors. The Juett et al. (2006) values are known most accurately, thus we use them throughout the rest

<sup>8</sup> <http://http://cxc.harvard.edu/ciao/threads>

of the paper.

In the two new *Chandra* observations, we detect several X-ray absorption lines. We define a detected line as one for which fits with a Gaussian give an equivalent width that excludes zero at more than the  $2\sigma$  level of confidence (note that we are being conservative by using the significance with which we can measure the equivalent width as the significance of the detection). In increasing wavelength (theoretical/best observational wavelengths are given in brackets), the detected lines are: Ne IX (13.447 Å), Ne III (14.508 Å), Ne II (14.608 Å), O VII (18.627 Å), O VIII (18.967 Å). All these absorption lines are detected in both observations, however, some were not detected in the previous *Chandra* observations, likely due to the lower sensitivity of those shorter observations. Whilst the O I absorption line at  $\sim 23.5$  Å was detected in all observations, we have not attempted to fit this line due to the complicated structure around this region due to multiple oxygen lines. The structure in this region has been studied in detail previously by Juett et al. (2004). The interstellar absorption at this wavelength also significantly increases the noise in the data, therefore the LETG observation of 4U 1820–30 previously studied present the best available dataset for analysis of this region. We also note that the O VII line at  $\sim 21.6$  Å was not detected in any of these observations, due to the low signal-to-noise in that region. Again, the previous LETG observation of 4U 1820–30 gives the best detection of this line.

In cases where an absorption line had been detected in one of the other observations, but not in the observation we were studying, a 95% confidence level upper limit for the line flux and equivalent width was determined. This was achieved by fixing the line wavelength at the theoretical value, fixing the width at a value smaller than the instrument resolution (as would be the case if the line was unresolved), and then increasing the line flux until the  $\chi^2$  value for the fit increased by 2.7. We justify fixing the width smaller than the instrument resolution as for the MEG, the resolution corresponds to a FWHM of  $\sim 350$  km s $^{-1}$  at 18.967 Å, and higher at shorter wavelengths. This is significantly higher than the expected thermal broadening in the ISM. Table 2 gives the line properties determined from the spectral fitting. In Fig. 1 we show the absorption lines detected in the two new *Chandra* observations.

As Ne IX is detected at 13.447 Å one should also expect to find additional Ne IX lines at 11.547 Å and 11.000 Å. However, we do not clearly detect these lines in any of the observations. If the line is not saturated, the ratio of the equivalent widths should follow the ratio of the oscillator strengths times the ratio of the wavelengths squared. The mean value of the equivalent width of the Ne IX (13.447 Å) line is approximately 5 mÅ. From the oscillator strengths, this would put the expected equivalent widths for the Ne IX lines at 11.547 Å and 11.000 Å to be 0.8 mÅ and 0.3 mÅ, respectively. In ObsId 6633, we note that there may be a weak absorption line present at  $\lambda = 11.550 \pm 0.007$  Å, with an equivalent width of  $EW = 1.8 \pm 0.9$  mÅ, though this is only a  $2\sigma$  detection. This measured equivalent width is consistent with what is predicted from the oscillator strengths. The line at 11.000 Å is not detected, and we determine the 95% confidence level upper limit to be 1.7 mÅ – the line would be too weak to detect given the noise in the data. In ObsId 6634 these Ne IX lines are not detected, and we find the upper limits on the

equivalent width for the lines at 11.547 Å and 11.000 Å to be 1.6 mÅ and 1.3 mÅ respectively, consistent with what would be expected from the oscillator strengths. We do not determine upper limits for these lines from the ObsId 1021 and 1022 datasets, as they are substantially less sensitive, and therefore the lines could not be detected at the predicted equivalent widths. While the upper limits do not rule out that the line is saturated, we cannot be conclusive.

Similarly, we try to determine whether the O VIII lines are saturated by determining limits on the O VIII Ly $\beta$  line at 16.006 Å. Fitting a Gaussian, with central wavelength fixed at 16.006 Å to ObsId 6633 and 6634 we measure equivalent widths of  $3.0 \pm 1.5$  mÅ, and  $3.4 \pm 2.8$  mÅ respectively. This gives the ratio of the equivalent widths of the O VIII Ly $\beta$  to Ly $\alpha$  as  $0.47 \pm 0.32$  and  $0.18 \pm 0.16$  for ObsId 6633 and 6634 respectively. For comparison, if the lines are not saturated we would expect this ratio to be 0.14 given the oscillator strengths and wavelengths. The measured value from ObsId 6634 is clearly consistent with this ratio, and in ObsId 6633 the ratio is not significantly different. However, as for Ne IX, we cannot rule out that the line is saturated.

#### 4.2. Source flux

In order to compare absorption line properties with the source properties, we determine the source flux from the best fitting continuum model to the HEG spectrum. For this broadband spectral fitting we use XSPEC (Arnaud 1996). We do not fit the MEG and HEG simultaneously due to the significant pileup in the first two observations, where the observations were not operated in continuous clocking mode. As the MEG has a larger effective area than the HEG at low energies (by about a factor of 2) it is more substantially affected by pileup. This is clearly apparent when trying to fit a continuum model to just the MEG spectra in these observations. There is an excess of counts at high energies and deficit at low energies, as expected by pileup. The HEG is much less affected, and thus we choose to fit to just the HEG 1st order spectra. For consistency, we use this method for fitting to the new *Chandra* observations also, even though they do not suffer from pileup.

We choose to fit an absorbed blackbody plus power-law model to the HEG spectra over the energy range 1.2–8 keV with the column density is fixed at the galactic value towards this globular cluster for all observations. Models to neutron star X-ray binary spectra can be degenerate (Lin et al. 2007), especially over a short energy range, such as covered by the HEG. The model we adopt is fiducial and reflects a physically-motivated scenario consisting of thermal and non-thermal emission. It allows us to characterize the source flux well because it provides a good fit to the spectrum. Importantly, it is a simple continuum model and so is easily reproducible, but, due to modeling degeneracies the specific parameter values derived should be regarded with caution. The fitted spectral parameters are given in Table 3.

We determine the 0.5–10 keV source flux, by extending a dummy response to lower and higher energies. We determine the uncertainty in the flux by propagating the errors on the individual parameters. The calculated fluxes are given in Table 3. We note that the uncertainties in the fluxes may be dominated by calibration uncertainties, and could be closer to around 6% (the difference in flux we find between fitting to the MEG and HEG) than those we determine from spectral fitting.

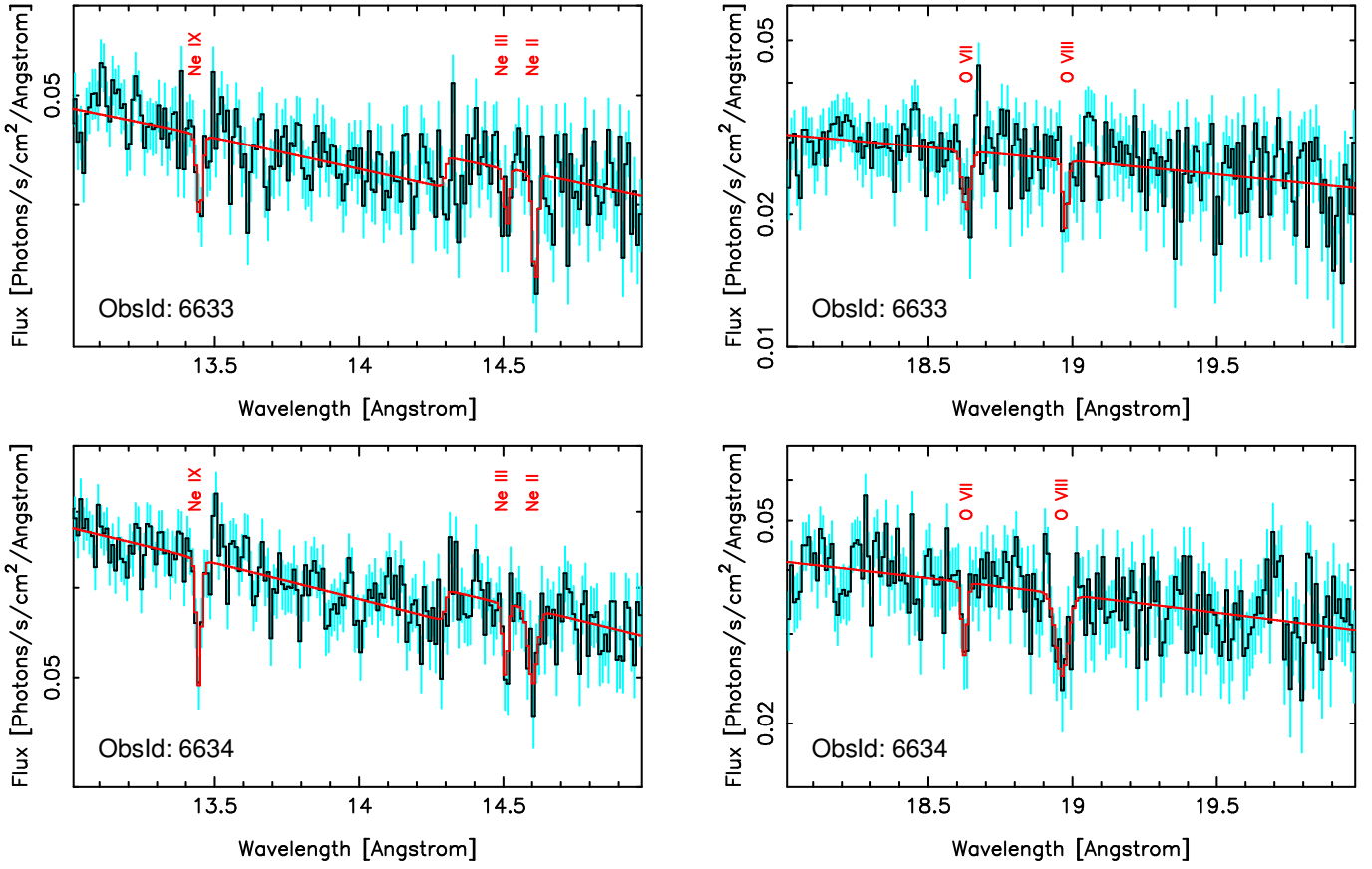


FIG. 1.— 13–15Å and 18–20Å segments of the combined first-order MEG spectra of 4U 1820–30. For illustrative purposes the data have been rebinned by a factor of 2. The top panels show these regions in ObsId 6633, and the bottom panels show these regions in ObsId 6634. The data is in black, and the  $1\sigma$  error bars are in blue. The best-fitting model is in red. The continuum is fit by a power-law modified by neutral ISM absorption edges, where appropriate. Absorption lines are modeled by a Gaussian. Table 2 gives the line properties.

We check whether pileup alters the determined fluxes substantially by comparing the calculated source fluxes with the 1-day average *RXTE* All-Sky Monitor (ASM) count rate for the day of each *Chandra* observation (see Tab. 3). Comparing the source flux against the ASM count rate, they are seen to be correlated, with no large offsets (see Fig. 2).

To look for variability of the absorption lines between each epoch, in Fig. 3 we plot the measured equivalent width (or upper limit, if the line is not detected) for each observation vs the 0.5–10 keV unabsorbed source flux (see Table 3). The errorbars indicate  $1\sigma$  uncertainties in the equivalent width. The dashed lines indicate the weighted mean (weighted by the uncertainties) of the equivalent widths of the detected lines. Generally, the equivalent widths of the lines are consistent between the observations. However, we note that the O VIII line does seem to display variability, although the variability is not highly significant and does not appear to be correlated with the source flux (see Fig. 3). The observed wavelength of the O VIII line is also found to be consistent with the theoretical wavelength and not blueshifted.

We calculate the  $\chi^2$  value for a fit of the equivalent widths for the O VIII line to their weighted mean to assess the significance of this variability. For the non-detection in ObsId 1021, we use the equivalent width determined from fitting a Gaussian fixed at the wavelength of the line in the calculation. This equivalent width is found to be  $2.9 \pm 2.9$  mÅ. We

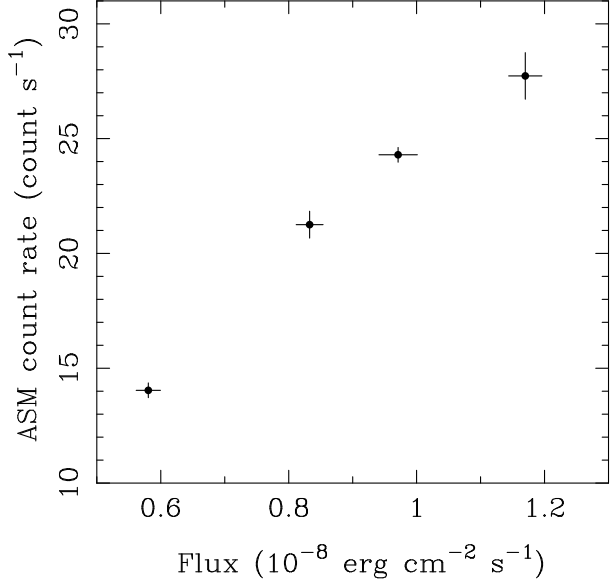


FIG. 2.— 0.5–10 keV unabsorbed source flux determined from fitting to the HEG spectra is shown versus the 1-day average *RXTE* All-Sky Monitor count rate on the day of each observation.

get  $\chi^2 = 14.1$  (3 degrees of freedom) when fitting the equivalent widths to their weighted mean. For the hypothesis that

TABLE 2  
ABSORPTION LINE PROPERTIES IN 4U 1820–30

ObsID	Ion	Transition	Theoretical (Å)	Observed (Å)	Equivalent width (mÅ)	FWHM (mÅ)	Flux ( $10^{-4}$ photons cm $^{-2}$ s $^{-1}$ )
1021	Ne IX	1s $^2$ –1s2p	13.447	13.455 $\pm$ 0.003	7.3 $\pm$ 1.8	3.8 $^{+7.3}_{-3.5}$	4.3 $\pm$ 1.0
	Ne III	1s–2p	14.508		< 3.7		< 2.1
	Ne II	1s–2p	14.608		< 8.1		< 4.7
	O VII	1s $^2$ –1s3p	18.627		< 10.2		< 4.8
	O VIII	1s–2p	18.967		< 10.8		< 4.8
1022	Ne IX	1s $^2$ –1s2p	13.447	13.448 $\pm$ 0.005	6.4 $\pm$ 2.2	19.3 $\pm$ 10.9	5.2 $\pm$ 1.8
	Ne III	1s–2p	14.508		< 3.5		< 2.7
	Ne II	1s–2p	14.608		< 3.6		< 2.8
	O VII	1s $^2$ –1s3p	18.627		< 6.6		< 6.0
	O VIII	1s–2p	18.967	18.966 $\pm$ 0.007	22.7 $\pm$ 6.3	33.4 $\pm$ 14.1	1.4 $\pm$ 0.4
6633	Ne IX	1s $^2$ –1s2p	13.447	13.450 $\pm$ 0.002	4.0 $\pm$ 0.9	1.4 $^{+9.7}_{-1.4}$	2.9 $\pm$ 0.7
	Ne III	1s–2p	14.508	14.505 $\pm$ 0.006	3.5 $\pm$ 1.3	18.6 $\pm$ 13.5	2.5 $\pm$ 0.9
	Ne II	1s–2p	14.608	14.611 $\pm$ 0.002	5.1 $\pm$ 1.2	0.07 $^{+11.6}_{-0.07}$	3.5 $\pm$ 0.8
	O VII	1s $^2$ –1s3p	18.627	18.634 $\pm$ 0.006	9.8 $\pm$ 3.0	24.0 $\pm$ 11.0	6.3 $\pm$ 2.0
	O VIII	1s–2p	18.967	18.972 $\pm$ 0.006	6.4 $\pm$ 2.9	7.1 $^{+21.2}_{-7.1}$	4.1 $\pm$ 1.8
6634	Ne IX	1s $^2$ –1s2p	13.447	13.445 $\pm$ 0.002	5.0 $\pm$ 0.8	1.4 $^{+8.6}_{-1.4}$	4.9 $\pm$ 0.8
	Ne III	1s–2p	14.508	14.508 $\pm$ 0.003	3.1 $\pm$ 1.1	3.2 $^{+13.0}_{-3.2}$	3.0 $\pm$ 1.0
	Ne II	1s–2p	14.608	14.602 $\pm$ 0.005	5.4 $\pm$ 1.2	27.8 $^{+12.2}_{-12.2}$	5.1 $\pm$ 1.2
	O VII	1s $^2$ –1s3p	18.627	18.625 $^{+0.007}_{-0.001}$	7.0 $\pm$ 2.5	0.02 $^{+14.4}_{-0.02}$	6.1 $\pm$ 2.3
	O VIII	1s–2p	18.967	18.965 $\pm$ 0.006	18.4 $\pm$ 4.5	45.9 $\pm$ 12.6	16.0 $\pm$ 4.0

NOTE. — See text for details on spectral fitting procedure. Theoretical line wavelengths for Ne IX, O VII, and O VIII are from Verner, Verner, & Ferland (1996). The line wavelengths for Ne II and Ne III are the best observationally determined values from Juett et al. (2006). Uncertainties and upper limits are  $1\sigma$  confidence limits. Where the line was not detected and we determine upper limits, the wavelength was fixed at the theoretical value, and the width of the Gaussian fixed below the instrument resolution.

TABLE 3  
SPECTRAL FITS TO 4U 1820–30

ObsID	Blackbody		Power-law		$\chi^2_\nu$	0.5–10 keV unabsorbed flux ( $10^{-9}$ erg cm $^{-2}$ s $^{-1}$ )	RXTE/ASM count rate (counts s $^{-1}$ )
	kT (keV)	Normalization	Spectral index	Normalization			
1021	0.72 $\pm$ 0.07	(3.5 $\pm$ 0.6) $\times$ 10 $^{-3}$	1.67 $\pm$ 0.02	0.85 $\pm$ 0.02	0.87	5.8 $\pm$ 0.2	14.0 $\pm$ 0.3
1022	0.96 $^{+0.15}_{-0.11}$	(4.5 $\pm$ 1.0) $\times$ 10 $^{-3}$	1.46 $\pm$ 0.02	1.13 $\pm$ 0.02	0.88	9.7 $\pm$ 0.3	24.3 $\pm$ 0.3
6633	1.16 $\pm$ 0.02	(2.1 $\pm$ 0.1) $\times$ 10 $^{-2}$	1.76 $\pm$ 0.03	1.12 $\pm$ 0.01	0.94	8.3 $\pm$ 0.2	21.3 $\pm$ 0.6
6634	1.20 $\pm$ 0.02	(3.2 $\pm$ 0.2) $\times$ 10 $^{-2}$	1.74 $\pm$ 0.02	1.50 $\pm$ 0.01	1.24	11.7 $\pm$ 0.3	27.7 $\pm$ 1.0

NOTE. — In all fits the column density was fixed at the cluster value of  $N_H = 1.5 \times 10^{21}$  cm $^{-2}$ . We used the XSPEC blackbody model named bbody, where the normalization is defined as  $L39/(D10)^2$ , where L39 is the luminosity in units of 10 $^{39}$  erg s $^{-1}$  and D10 the distance to the source in units of 10 kpc. The power-law normalization is defined at 1 keV, with units of photons keV $^{-1}$  cm $^{-2}$  s $^{-1}$ . The spectral fits are to the HEG 1st order spectrum (see text for details). For comparison with the source flux, the RXTE/ASM count rate for 4U 1820–30 is also given.

the equivalent widths are constant, this corresponds to a probability for achieving a higher  $\chi^2$  value of 0.003. However, we note that we have searched 5 lines to find variability of this level, and thus this increases the probability to 0.015. This is equivalent to the line being variable at the  $2.4\sigma$  level of confidence. Thus, while it is not a highly significant result, low-level variability cannot be ruled out for this line.

In comparing equivalent width measurements from multiple epochs, it is important to consider whether any systematic effects can cause variability in the lines. Importantly, neither the first two observations (ObsId 1021 and 1022) were operated in continuous-clocking mode, and thus both are affected by pileup. It is not clear how pileup alters equivalent width measurements, though we note that as the O VII and O VIII lines are close together in wavelength they should be affected similarly. Any effect must be fairly small, as the O VIII line is seen to vary whereas the O VII is not.

## 5. DISCUSSION

We have analyzed four *Chandra* HETGS observations of the neutron star low-mass X-ray binary 4U 1820–30 and detect a variety of absorption lines in the spectra. To investigate the nature of these lines, we compare the line equivalent widths between the observations. If the line is unsaturated and on the linear part of the curve of growth, then the equivalent width is a direct measure of the absorbing column. If the equivalent width does not vary between observations, this would therefore indicate that the absorbing column has remained unchanged between the observations, as would be expected for absorption lines associated with the ISM. The majority of the absorption lines present in 4U 1820–30 are consistent with remaining constant between the observations, suggesting they are interstellar in origin. However, if the lines are saturated, then even if the column density changes significantly (for instance in response to changes in the source) the equivalent width would remain more or less constant. Moreover, if the lines are interstellar in origin, then we might expect the lines to be fairly narrow ( $\sim$ 100 km s $^{-1}$ ) based on the narrow widths of O VI lines observed in the ISM

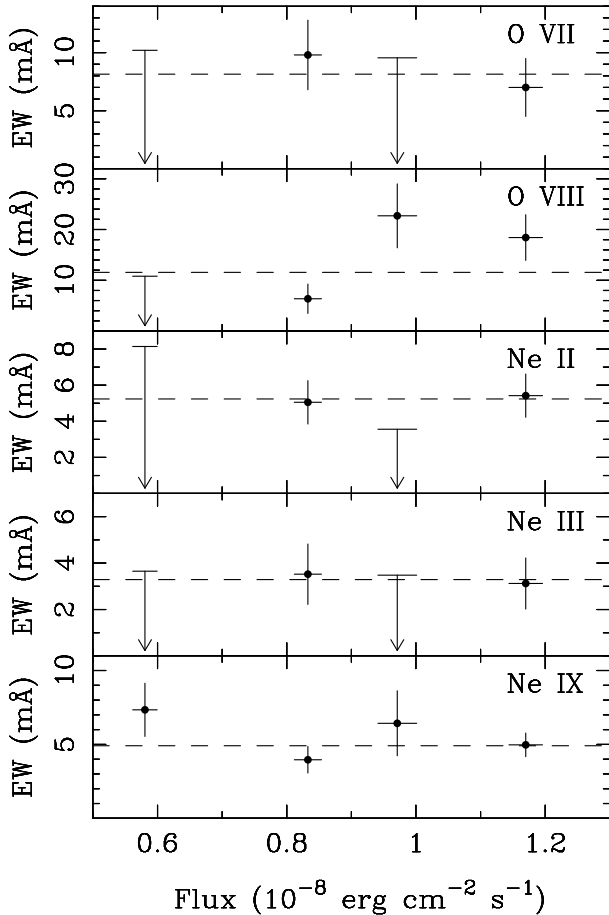


FIG. 3.— Equivalent widths (mÅ) of the various absorption lines in 4U 1820–30 versus 0.5–10 keV unabsorbed source flux in units of  $10^{-8}$  erg  $cm^{-2}$   $s^{-1}$ . Dashed lines indicate the weighted mean of the measured equivalent widths. Arrows indicate 95% confidence upper limits and errorbars indicate  $1-\sigma$  uncertainties.

(Savage et al. 2003; Savage & Lehner 2006). In this case one would need a large column density and a saturated line to reach the observed equivalent widths. However, if the lines

are formed in an accretion disk wind or corona, it is conceivable that the line widths are higher and thus the observed equivalent widths can be achieved with unsaturated or only mildly saturated lines. Unfortunately, from upper limits on the Ne IX and O VIII Ly $\beta$  lines we cannot conclusively determine whether or not the lines are saturated.

Additionally, if the absorption lines were associated with a disk wind, then blueshifts would be expected. We find that the wavelength of the absorption lines are consistent with their rest wavelengths (after accounting for the absolute instrumental calibration uncertainty of 0.05%), as expected for interstellar lines. However, we note that in the dipping X-ray binaries, absorption lines that are local to the source are not seen to be blueshifted and are thought to be associated with the accretion disk corona rather than an accretion disk wind. Similarly, here the lack of blueshifts could just be explained by absorption from an accretion disk corona (Díaz Trigo et al. 2006).

We find that there may be a low level of variability in the O VIII Ly $\alpha$  line, which may indicate it is associated with the source. If the absorption is local to the source, this variability could be, for example, due to changes in mass accretion rate leading to changes in mass outflow. If one naively assumes that the continuum flux traces the mass accretion rate one would therefore see correlated variability between the source flux and the line equivalent width. Alternatively, if the properties of the absorbing column are approximately constant and the ionizing flux changes, the fraction of oxygen in O VIII should change, which could lead to correlated variability. However, there appears to be no such correlation observed (see Fig. 3) though more observations are required to be conclusive.

We conclude that a high fraction of the absorption 4U 1820–30 is interstellar in origin although further sensitive observations of this source are needed to confirm variability in the O VIII line, and search for low-level variability in other lines.

We thank the *RXTE/ASM* team for the quick-look results used in this paper. JMM gratefully acknowledges support from Chandra.

## REFERENCES

Arnaud, K. A. 1996, in ASP Conf. Ser. 101: Astronomical Data Analysis Software and Systems V, 17

Behar, E. & Netzer, H. 2002, ApJ, 570, 165

Bohlin, R. C., Savage, B. D., & Drake, J. F. 1978, ApJ, 224, 132

Boirin, L., Méndez, M., Díaz Trigo, M., Parmar, A. N., & Kaastra, J. S. 2005, A&A, 436, 195

Chelouche, D. & Netzer, H. 2005, ApJ, 625, 95

Church, M. J., Reed, D., Dotani, T., Bałucińska-Church, M., & Smale, A. P. 2005, MNRAS, 359, 1336

Cottam, J., Kahn, S. M., Brinkman, A. C., den Herder, J. W., & Erd, C. 2001a, A&A, 365, L277

Cottam, J., Sako, M., Kahn, S. M., Paerels, F., & Liedahl, D. A. 2001b, ApJ, 557, L101

Díaz Trigo, M., Parmar, A. N., Boirin, L., Méndez, M., & Kaastra, J. S. 2006, A&A, 445, 179

Dickey, J. M. & Lockman, F. J. 1990, ARA&A, 28, 215

Futamoto, K., Mitsuda, K., Takei, Y., Fujimoto, R., & Yamasaki, N. Y. 2004, ApJ, 605, 793

Juett, A. M., Schulz, N. S., & Chakrabarty, D. 2004, ApJ, 612, 308

Juett, A. M., Schulz, N. S., Chakrabarty, D., & Gorcey, T. W. 2006, ApJ, 648, 1066

Kuulkers, E., den Hartog, P. R., in't Zand, J. J. M., Verbunt, F. W. M., Harris, W. E., & Cocchi, M. 2003, A&A, 399, 663

Lee, J. C., Reynolds, C. S., Remillard, R., Schulz, N. S., Blackman, E. G., & Fabian, A. C. 2002, ApJ, 567, 1102

Lin, D., Remillard, R. A., & Homan, J. 2007, ArXiv Astrophysics e-prints, astro-ph/0702089

Miller, J. M., Raymond, J., Fabian, A., Steeghs, D., Homan, J., Reynolds, C., van der Klis, M., & Wijnands, R. 2006a, Nature, 441, 953

Miller, J. M., Raymond, J., Fabian, A. C., Homan, J., Nowak, M. A., Wijnands, R., van der Klis, M., Belloni, T., Tomsick, J. A., Smith, D. M., Charles, P. A., & Lewin, W. H. G. 2004, ApJ, 601, 450

Miller, J. M., Raymond, J., Homan, J., Fabian, A. C., Steeghs, D., Wijnands, R., Rupen, M., Charles, P., van der Klis, M., & Lewin, W. H. G. 2006b, ApJ, 646, 394

Parmar, A. N., Oosterbroek, T., Boirin, L., & Lumb, D. 2002, A&A, 386, 910

Savage, B. D. & Lehner, N. 2006, ApJS, 162, 134

Savage, B. D., Sembach, K. R., Wakker, B. P., Richter, P., Meade, M., Jenkins, E. B., Shull, J. M., Moos, H. W., & Sonneborn, G. 2003, ApJS, 146, 125

Schulz, N. S., Chakrabarty, D., Marshall, H. L., Canizares, C. R., Lee, J. C., & Houck, J. 2001, ApJ, 563, 941

Sidoli, L., Oosterbroek, T., Parmar, A. N., Lumb, D., & Erd, C. 2001, A&A, 379, 540

Stella, L., Priedhorsky, W., & White, N. E. 1987, ApJ, 312, L17

Ueda, Y., Murakami, H., Yamaoka, K., Dotani, T., & Ebisawa, K. 2004, ApJ, 609, 325

Verner, D. A., Verner, E. M., & Ferland, G. J. 1996, Atomic Data and Nuclear Data Tables, 64, 1

Yao, Y. & Wang, Q. D. 2005, ApJ, 624, 751

—. 2006, ApJ, 641, 930